XXXVII SIMPÓSIO BRASILEIRO DE TELECOMUNICAÇÕES E PROCESSAMENTO DE SINAIS - SBrT2019, 29/09/2019–02/10/2019, PETRÓPOLIS, RJ

Modeling and Characterization of a Holographic Artificial Impedance Antenna with SIW feeding for Frequency-controlled Beam Scanning

Yoiz E. Nuñez, Johnes R. Gonçalves, Marbey M. Mosso and Glaucio L. Siqueira

***Abstract*— In this work is proposed a Holographic Artificial Impedance Antenna (HAIA) implemented with a Substrate Integrated Waveguide (SIW) feeding to produce a narrow beam in a controlled direction. Parameters in the feeding such as directivity, Front-to-Back Ratio (FTBR) and reflection coefficient (S_{11}) can be engineered to provide a surface wave more directive, exciting the antenna with a higher level of power. The results present that the dimension of the holographic surface can be reduced without affects the performance in relation to high gain, low side lobe level, and narrow beam. Furthermore, a modification in the holographic surface was realized producing a change in the polarization of the antenna.**

***Keywords*— Leaky wave, SIW feeding, Impedance surface.**

I. Introduction

HAIAs belong to a group of leaky wave antennas characterized by the conversion of a surface wave mode into a leaky-wave mode to generate controlled beam radiation in the far-field [1]. The contributions around the world about this topic have increased by their uniqueness and relevant principle operation. Those antennas are known for their high gain, narrow beamwidth, and beam scanning capability without complex feed network such as phased array system [2], composed of two parts: holographic artificial impedance and surface wave feeding.

Artificial impedance Surface (AIS) has been defined in some literature as two-dimensional (2D) version of metamaterials [1],[3] with subwavelength thickness known as metasurface, providing control of polarization, phase, and amplitude of the incident wave. For application in antennas, D. Sievenpiper in [4] developed a method with scalar and tensorial impedance producing linear and circular polarization, respectively, using the theory of impedance modulation [5] and the holographic principle applied in optic systems, creating a new type of antenna with control of the desired radiation angle.

The classical design of the HAIAs has used a monopole or dipole to generate a surface wave mode. Recently, other types of feedings as planar source integrated directly in the dielectric substrate are of interest for a design more compact, easy integration to the holographic pattern for operation up to high-frequency [2], allowing reduce the size of the antenna without affects its performance.

Yoiz E. Nuñez, Johnes R. Gonçalves, Marbey M. Mosso and Glaucio L. Siqueira, Center of study in telecommunications PUC-Rio, street Marquês de São Vicente, 225 - Ala Kennedy - 7º andar - Gávea - CEP 22451-900 - Rio de Janeiro - RJ, e-mail: yoiz.nunez@cetuc.puc-rio.br. This work was partilly supported by CNPq.

In this work, a surface wave feeding based in the SIW technology for the operating frequency of 18.4 GHz is proposed with potential application in the Ku and K bands for radar and satellites systems. The holographic artificial impedance was developed with scalar impedance for the excitation of a TM mode in the surface. Thus, an electric field polarized linearly is radiated far away from the antenna, where modifying the distribution of the impedance surface as shown in [1] was also changed the polarization of the antenna without affecting the rest of the structure.

II. Holographic Artificial Impedance Surface

The modeling of the holographic antenna starts with the design of the unit cell to find the impedances values that will be distributed over the surface. The scalar impedance boundary is given by

$$E = Z_s J, \tag{1}$$

where E is the electric field, Z_s is the impedance surface and J is the surface current.

A. *Design of the unit cell*

AIS uses a periodic array of geometries with dimensions smaller that the wavelength. Due to this periodicity, the analysis of the AIS can be made with a single unit cell of length a conformed by a square patch over a grounded dielectric substrate as illustrated in figure 1, producing a scalar capacitive impedance [13] to propagate a TM mode along the surface. In the design was used a dielectric substrate RT/duroid 5880 with electric permittivity ϵ_r= 2.2, loss tangent tanδ = 0.0009, thickness cooper of 0.035 mm and height of 1.57 mm.

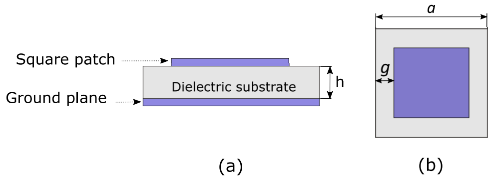

Fig. 1. AIS unit cell: (a) frontal view, and (b) superior view.

The design goal of the unit cell is to provide high impedance values with changes in each variation of the square metal sizes defined by the gaps g. For obtaining the impedance values of the geometry was used the method developed in [4], where a unit cell is characterized with periodic boundary conditions Master/Slave using the *eigenmode* function on HFSS (High Frequency Structure Simulator) to find the frequencies of ressonance and resolve the refractive index n in the surface. The resulting curve of impedance is shown in figure 12, with values between 160.18 jΩ and 245.46 jΩ.

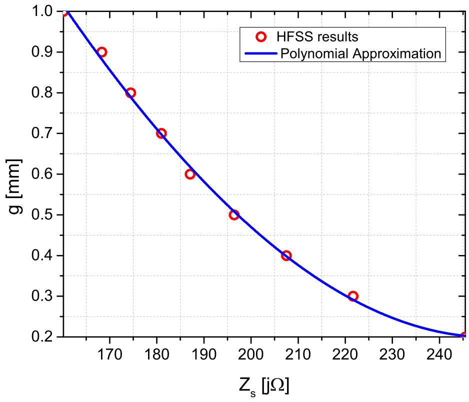

Fig. 2. Impedance curve of the AIS unit cell.

A polynomial approximation was calculated to obtain the relationship between the impedance Z_s and the gaps g, given by the equation (2). This is useful to make the hologram impedance distribution detailed in the following section.

$$g = -2.83^{-7}(Z_s^3) + 2.72^{-4}(Z_s^2) - 0.08(Z_s) + 8.83. \quad (2)$$

B. Holographic principle

The holographic principle for its application in antennas is implemented in the same way that optical systems, consisting of two steps: recording and reconstruction of the object. A source feeding generates a surface wave ($\Psi_{surf} = e^{-jknr}$) regarded as the reference wave and the desired radiation pattern is the object wave ($\Psi_{rad} = e^{-jk_x sin(\theta_m)}$) [4] where k is the propagation constant, n is the effective index seen by the surface currents and r is the distance from the position of the feeding. The desired field is defined to radiate in a specific angle (θ_m) in the plane XZ, both information is recorded in the hologram, as shown in figure 3. When the surface wave is excited in the holographic artificial impedance, it will be radiated the desired field, expressed by

$$(\Psi_{rad}\Psi^*_{surf})\Psi_{surf} = \Psi_{rad}|\Psi_{surf}|^2. \quad (3)$$

The information of the surface wave and the desired radiation pattern is recorded in the hologram using a sinusoidal modulation defined by [5]

$$Z_s = j[X + MRe(\Psi_{rad}\Psi^*_{surf})], \quad (4)$$

where X is an average value of the impedance distribution, M is the factor of modulation. Thus, using the equation (2) and (4) is possible to make a systematic and smart distribution of the impedance, because if it knows the surface wave that

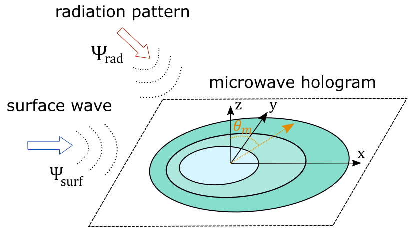

Fig. 3. Illustration of a microwave hologram.

is being excited and the desired field, it would be known the necessary distribution of impedance for convert a surface wave into a leaky-wave in a controlled radiation. The resulting hologram is formed by concentric ellipses of metal patches as illustrated in figure 4. The smallest square presents high values of impedance.

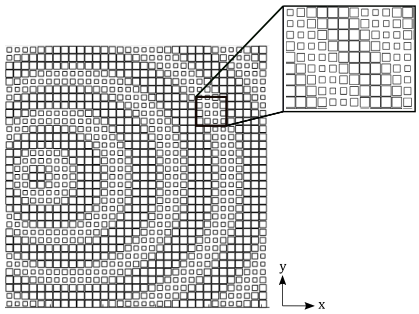

Fig. 4. Holographic pattern conformed by a variation of square patches.

III. Surface Wave Feeding

Feeding with a direct planar source such as a Microstrip transmission line [7], Slotted quasi-Yagi-Uda [8], Antipodal Feed for frequency scanning Radar [9] can produce a surface wave. Another planar launcher is a SIW H-plane sectoral, used in this project by its simple design widely studied in the literature [2], [10], [11], and easy integration with the holographic surface .

In leaky-wave antennas, the surface wave needs a surface with an adequate length to be propagated; this changes to the type of feeding. When the surface area is reduced, the performance of the antenna in the desired beam angle is affected. To obtain a narrow beam with a gain higher than 20 dB was reported in [4] a holographic surface of 40.64 cm x 25.4 cm and in [1] was used a dimension of 23.87 cm x 19.81 cm for a gain of 16 dB , both with a monopole feeding. SIW feeding was studied and designed presenting the following advantages:

- An excitation of the surface wave more directive, exciting the antenna with a high level of power,
- To allow the reduction of the area in the holographic surface without affecting the performance of the antenna.

A. SIW H-plane sectoral feeding

The development of the SIW technology since its invention in 2001 [10] allowed a new type of H-plane sectoral antenna based in that approach. The structure is composed by a rectangular waveguide formed by cylinder metal post (vias) embedded in a dielectric substrate acting as electric walls to generate the propagation of a guide mode with an aperture waveguide in the direction of the magnetic field, following the same rules of the conventional H-plane Horn antennas [2].

This type of feeding operating in millimeter waves presents poor radiation when the thickness of the substrate is smaller than the wavelength. Also, frequencies below of 20 GHz with substrates smaller than $\lambda/6$ present a mismatch in the output of the feeding, producing unwanted back radiation. These limitations can be overcome with a practical solution described in [10] and [11] using a printed transition zone after the aperture of the feeding to improve the parameter of Front-to-back Ratio (FTBR), keeping the compact design and easy implementation. A basic transition zone consists of two parallel blocks printed on the copper layer of the substrate, seen as radiating elements, other shapes, such as rectangles or triangles, can also be used to improve performance parameters, and the number of elements depends on the opening waveguide. The SIW propose is shown in the figure 5(a). In addition, a monopole of a quarter-wavelength was used for a comparative analysis as illustrated in the figure 5(b) with d_m = 0.3 mm.

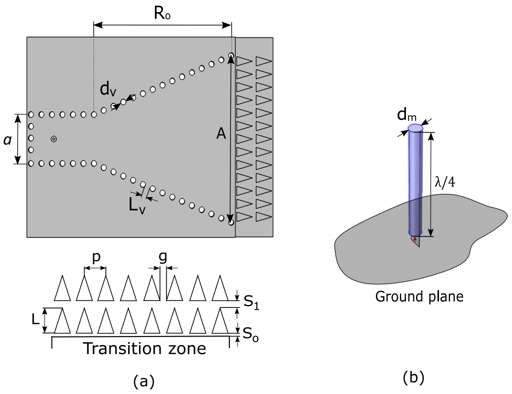

Fig. 5. Structure of the feeding: (a) SIW H-sectoral, and (b) Monopole of a quarter-wavelength.

The cutoff frequency of propagating modes within the guide is defined by:

$$f_{mn} = \frac{\pi}{\sqrt{\mu\epsilon}}\sqrt{\frac{m^2}{a^2}+\frac{n^2}{b^2}}, \quad (5)$$

where a and b are the width and height of the waveguide, μ and ϵ are the permeability and permittivity of the substrate, respectively. Within the guide, m and n are related to propagation modes. The modes allowed are the $TE_{n0}, (n = 1, 2...)$, where the fundamental mode is TE_{10}. Due to the gap between the metalized vias, the transverse magnetic mode (TM) is not supported [12]. To ensure the existence of a single propagation mode inside the structure, the width a must have to:

$$\frac{\lambda_o}{2\sqrt{\epsilon_r}} < a < \frac{\lambda_o}{\sqrt{\epsilon_r}}. \quad (6)$$

Thus, for the mode fundamental (f_{10}), the equation (6) is reduced in [12]

$$f_{10} = \frac{c_o}{2\sqrt{\epsilon_r}a}. \quad (7)$$

An effective width w_{eff} is calculated [10] to relate the characteristics of the conventional waveguide with the SIW expressed by

$$w_{eff} = a - \frac{d_v^2}{0.95L_v}, \quad (8)$$

where a is the distance between the walls of the waveguide, d_v is the diameter of the metalized vias and L_v is the gaps between them. To avoid leakage energy between the vias is recommended values of $d_v/L_v < 2.5$. The parameters A and R_o determines the gain and the aperture pattern of the feeding as in the classical H-sectoral antenna. In [12] are presented the curves of gain for SIW H-sectoral antennas. In this work, for modeling the waveguide was chosen the frequency of the fundamental mode (f_{10}) to be 13 GHz.

The optimized values of the transition zone are: L = 3mm, p = 2.2mm, g = 0.6 mm, S_1 = 0.7 mm and S_o = 0.2mm resolved in the simulation of HFSS. To generate the TE_{10} mode inside the guide, was used a coaxial probe with a inner and outer conductor of 0.38 mm and 3.5 mm of diameter respectively. The distribution of the electric field and radiation pattern 3-D in the frequency of 18.4 GHz is presented in the following figure. The FTBR obtained was 32.12 dB with a S_{11} of -31.64 dB. The distribution of the electric field and gain in the frequency of 18.4 GHz is presented in the figure 6.

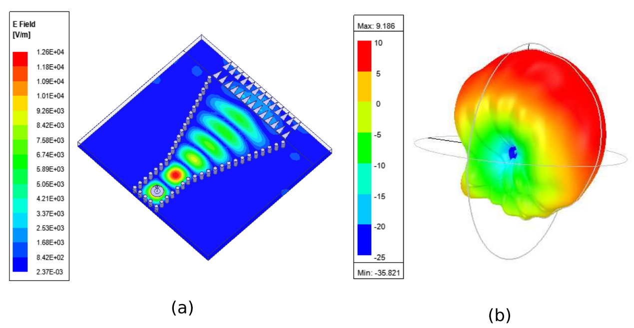

Fig. 6. SIW structure (a) distribution electric field (b) radiation pattern 3-D. The dimension of the structure are: w_{eff} = 8.3 mm, a = 7.3 mm, d_v = 1mm, L_v = 1 mm, A = 28.30 mm, R_o = 26.15 mm.

IV. Design of the Holographic Antenna

The holographic artificial impedance was made in the operating frequency of 18.4 GHz with dimensions $L_h = 20$ cm and W_h = 20 cm conformed by 4,489 square metal, distributed symmetrically on the surface to produce a main lobe in θ_m = 20°. In HFSS, the air box was configured with radiation boundary in a distance of λ from the structure and a ground plane was used in the entire structure. The designs are shown in figure 7. The S-parameter result of the SIW and monopole feeding is show in figure 8. The behavior of the SIW feeding when the holographic surface is added, keeps similar values of the feeding alone.

The radiation pattern in figure 9 was plotted for a XZ plane ($\phi = 0$) in E-plane and a XY plane ($\theta = \theta_m$) in

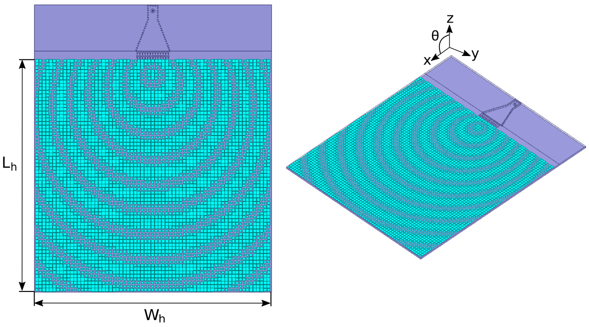

Fig. 7. Design of the holographic artificial impedance antenna.

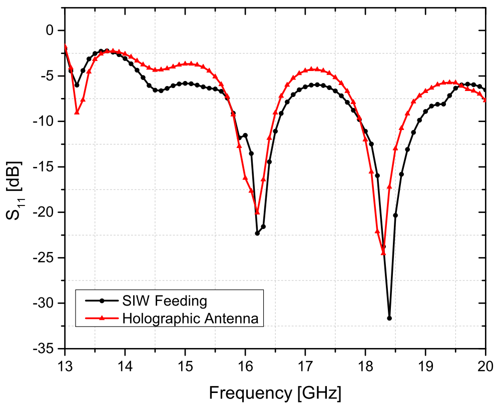

Fig. 8. S-parameter of the holographic antenna.

the H-plane. The main lobe radiate to 23° with a gain of 22.02 dB, HPBW (Half Power Beam Width) of 4.71° and side lobe level of -8.08 dB in the E-plane. The antenna radiates with low values in the H-plane showing a low cross-polarized component. The distribution of the intensity electric field and the surface current is presented in figure 10. A comparative result between feedings is presented in the radiation pattern of the figure 11. With the monopole, a split in the direction of the maximum lobe appeared [1] using the dimensions W_h = 20 cm and L_h = 20 cm. It was found that the phenomenon can disappear with a higher dimension of the holographic surface (25%). Therefore, the SIW feeding presents the best performance using smaller dimension, leading to a process of miniaturization. A variation of the operating frequency without modifying the structure was realized, showing the frequency-controlled beam scanning behavior as was expected. The maximum angle increase when the frequency is higher without an abrupt change of the gain. The values of gain and maximum angle of radiation corresponding to each frequency change is presented in figure 8. These range of frequencies show values of S_{11} less than -10 dB.

V. Holographic Antenna with Horizontal Polarization

Another feature in the holographic antenna using the method of Artificial Impedance Surface is the change to horizontal polarization developed in [13]. The hologram is designed

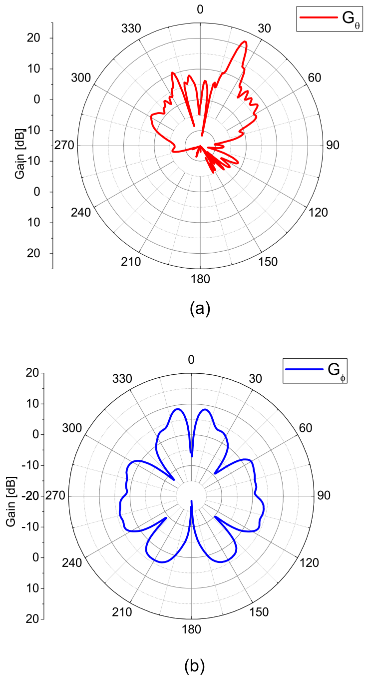

Fig. 9. Radiation pattern of the holographic antenna with SIW feeding (a) G_θ component along XZ plane (ϕ = 0°) (b) G_ϕ component along θ_m = 23°.

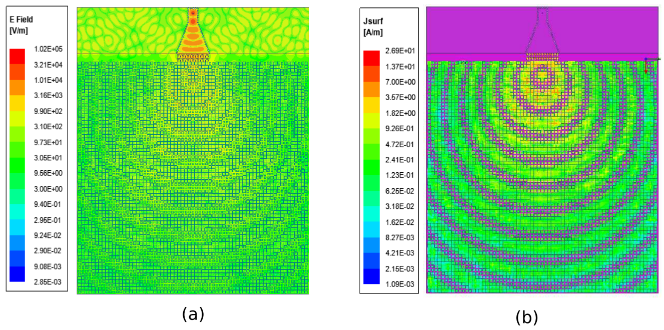

Fig. 10. Distribution of the (a) magnitude electric field (b) of the holographic antenna with SIW feeding.

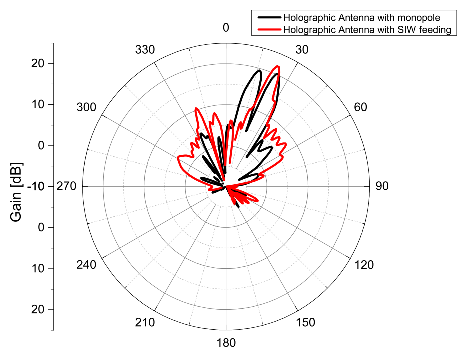

Fig. 11. Comparative in the G_θ component along XZ plane (ϕ = 0°).

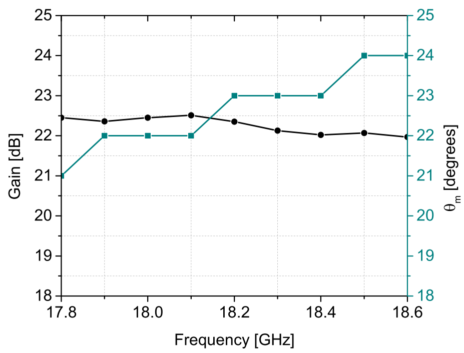

Fig. 12. Prototype antenna with SIW H-sectoral feeding.

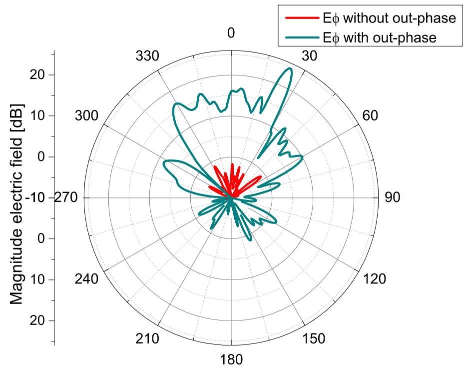

Fig. 14. Comparative radiation pattern of the magnitude electric field.

180° out-phase in one of its halves ($W_h/2$) to support the propagation of a TE surface wave mode to radiate the horizontally polarized electric field, as illustrated in figure 13. An improvement in the magnitude of the horizontal component of the electric field is generated. The equations for the impedance surface distribution in the modified holographic pattern are described below.

$$Z_{s1} = j[X + MRe(e^{-jk_x sin(\theta)} e^{jknr})], x < 0$$
$$Z_{s2} = j[X + MRe(e^{j\pi} e^{-jk_x sin(\theta)} e^{jknr})], x > 0. \quad (9)$$

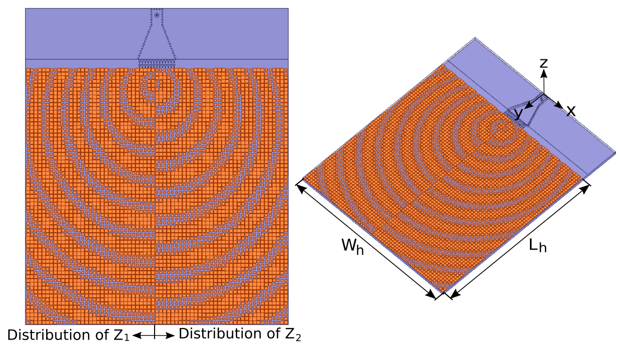

Fig. 13. Distribution of the current surface over the hologram.

The hologram out-phase was realized in the operating frequency of 18.4 GHz. The radiation pattern in the figure 14 shows the magnitude of the electric field in the H-plane, with and without out-phase, presenting an increase of the magnitude electric field with the modified surface.

VI. Conclusions

A Holographic Artificial Impedance antenna with a SIW feeding using a small triangles transition zone was proposed. High gain was obtained with a beam scanning behavior between 17.8 GHz to 18.6 GHz with S_{11} less than -10 dB. Increasing of 1° for every 0.3 MHz of increment was obtained, presenting a narrow beam and sidelobe levels less than 10 dB in relation with the main lobe. With the SIW feeding, the dimensions of the holographic surface can be reduced in a 25% without affects the performance of the antenna. Furthermore, a modification of the holographic surface was realized to improve the horizontal component of the electric field in the direction of the desired field with the design proposed.

Acknowledgements

The authors would like to thank the Center of study in telecommunications (CETUC) and CNPq for the financial support.

References

[1] PANDI, S.. Holographic metasurface leaky wave antennas. 2017.
[2] CHEN, Z. N.; LIU, D.; NAKANO, H.; QING, X. ; ZWICK, T.. Handbook of Antenna Technologies. Springer Publishing Company, Incorporated, 2016.
[3] RAMOS, W. T.; MESQUITA, R. C. ; SILVA, E. J.. Electric field distribution on surface of the artificial magnetic conductor: miniaturization process. In: METAMATERIALS, METADEVICES, AND METASYSTEMS 2017, volumen 10343, p. 1034326. International Society for Optics and Photonics, 2017.
[4] FONG, B. H.; COLBURN, J. S.; OTTUSCH, J. J.; VISHER, J. L. ; SIEVENPIPER, D. F.. Scalar and tensor holographic artificial impedance surfaces. IEEE Transactions on Antennas and Propagation, 58(10):3212?3221, 2010.
[5] OLINER, A.; HESSEL, A.. Guided waves on sinusoidally-modulated reactance surfaces. IRE Transactions on Antennas and Propagation, 7(5):201?208, 1959.
[6] Planar integrated holographic antenna with substrate integrated waveguide. https://pdfs.semanticscholar.org/ff1a/34d2a65a850ee0ac9a86e09dc0507cab546d.pdf.
[7] PATEL, A. M.; GRBIC, A.. A printed leaky-wave antenna based on a sinusoidally-modulated reactance surface. IEEE Transactions on Antennas and Propagation, 59(6):2087?2096, 2011.
[8] PODILCHAK, S. K.; FREUNDORFER, A. P. ; ANTAR, Y. M.. Surfacewave launchers for beam steering and application to planar leaky-wave antennas. IEEE Transactions on Antennas and Propagation, 57(2):355?363, 2009.
[9] RUSCH, C.; BEER, S.; GULAN, H. ; ZWICK, T.. Holographic antenna with antipodal feed for frequency-scanning radar. In: 2013 IEEE ANTENNAS AND PROPAGATION SOCIETY INTERNATIONAL SYMPOSIUM (APSURSI), p. 234?235. IEEE, 2013.
[10] ESQUIUS-MOROTE, M.; FUCHS, B.; ZÜRCHER, J.-F. ; MOSIG, J. R.. A printed transition for matching improvement of siw horn antennas. IEEE Transactions on Antennas and propagation, 61(4):1923? 1930, 2013.
[11] ESQUIUS-MOROTE, M.; FUCHS, B.; ZÜRCHER, J.-F. ; MOSIG, J. R.. Novel thin and compact h-plane siw horn antenna. IEEE Transactions on Antennas and Propagation, 61(6):2911?2920, 2013.
[12] BOZZI, M.; GEORGIADIS, A. ; WU, K.. Review of substrateintegrated waveguide circuits and antennas. IET Microwaves, Antennas and Propagation, 5(8):909?920, 2011.
[13] PANDI, S.; BALANIS, C. A. ; BIRTCHER, C. R.. Design of scalar impedance holographic metasurfaces for antenna beam formation with desired polarization. IEEE Transactions on Antennas and Propagation, 63(7):3016?3024, 2015.